Progress In Electromagnetics Research, PIER 80, 431–445, 2008

PHOTONIC CRYSTALS AS INFRARED BROADBAND REFLECTORS WITH DIFFERENT ANGLES OF INCIDENCE: A COMPARATIVE STUDY

N. Kumar

FASCL, Mody Institute of Technology & Science
Deemed University
Lakshmangarh, Sikar-332 311, Rajasthan, India

S. P. Ojha

CCS University
Meerut-250 005, India

Abstract—In this communication, we theoretically report the reflection properties of a photonic crystal with alternate layers of air and GaAs for specified values of the lattice parameters. By employing the transfer matrix approach, the reflection spectra of the layered media are obtained for chosen sets of number of unit cells and incident angles. It is observed that the photonic crystals with different number of unit cells completely reflect a wide band in the infrared region of radiation. Also, we find that the reflectivity decreases and the completely reflected bands are shifted towards lower wavelength side with increase in the incident angle. Further, the reflected broadbands in the reflection spectra correspond to the forbidden ranges of wavelength obtained by using the analogy of Kronig-Penney model. It indicates that the completely reflected ranges are forbidden bandgaps, which is considered as an important feature of the proposed photonic crystals.

1. INTRODUCTION

In recent years, photonic band gap (PBG) structures have generated a great deal of interest because of their peculiar optical properties such as abnormal refractive index, gain enhancement at the band edge and negative refraction [1–8]. Photonic crystals consist of periodic arrangements of materials with refractive indices of high contrast

ratio and exhibit bandgaps at optical frequencies in a similar manner as electron through periodic potential of semiconductors organize into electronic bands of various energies separated by bandgaps. These PBG materials are composed of air, dielectrics, semiconductors, polymers, and metals. By introducing a properly designed defect in a PBG structure, strong localization of photon waves in the region near defect is possible. The existence of the spectral gap in such photonic crystals opens up variety of potential applications in various optical devices. The photonic devices have great advantages over conventional electronic devices. These devices provide very high speed of operation, greater efficiency, and tolerance to temperature fluctuation [12]. In total, photonic crystals offer unprecedented control of light and show promise for their applications in several areas, including waveguides, biophotonic sensors, nanotechnology, integrated photonic chips, spontaneous emission, photon trapping, and biomedical optics. Many investigators have studied their various properties [9–38]. Yabolnovitch [8] introduced the photonic band gap for controlling spontaneous emission of light. Ojha et al. [11, 12] proposed optical filters using PBG materials. Omnidirectional reflections through photonic crystals have already been reported [13, 14]. Massaoudi et al. [26] demonstrated the properties of metallic PBG material with defect at microwave frequencies with experimental verification. Further, Villa-Villa et al. [27] showed the surface modes in one-dimensional (1-D) photonic crystals, that include left-handed materials. Structural parameters for the formation of 1-D photonic band gap in photonic crystal have recently been suggested by Singh et al. [28]. Yeh [15] formulated matrix approach for optical waves and reflection through layered media.

In this study, we have made an attempt to analyze the reflection properties of a PBG structure with refractive index profile of air and gallium arsenide GaAs for specified values of lattice parameters. We employ the transfer matrix approach suggested by Yeh et al. [15, 16] to obtain the reflectance of the photonic crystal, and reflection spectra are drawn for different number of unit cells: $N = 5$, 10, 17 with variation of the incident angle: $\theta = 0°$, 30°, 45°, and 60°. We observe from these reflection spectra that the proposed photonic crystals with different unit cells act as infrared broadband reflectors. The reflected broadbands in the reflection spectra are also compared with the forbidden bandgaps obtained using the analogy of Kronig-Penney model in the band theory of solids. Thus, this paper compares the reflectance of 1-D photonic crystal in different cases of unit cells and incident angles.

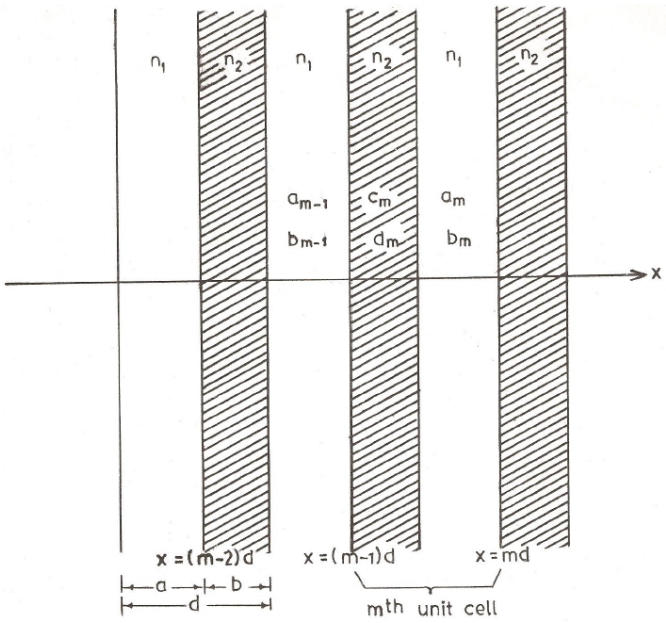

Figure 1. Geometry of a periodic refractive index profile in form of rectangular structure.

2. THEORETICAL FRAMEWORK

First, we consider the propagation of electromagnetic waves in a simple periodic layered media consisting of alternate layers of different refractive indices and assume that the material is non-magnetic. We employ the matrix formulation approach [15, 16] in order to study the reflection properties of the photonic crystal. Figure 1 shows the photonic crystal with a periodic refractive index pattern of the materials in the form of rectangular symmetry with its mth unit cell. Selecting a direction along x-axis through the structure normal to the layers, the periodic refractive index profile can be defined as

$$n(x) = \begin{cases} n_1, & b < x < d \\ n_2, & 0 < x < b \end{cases}, \tag{1}$$

where $n_1(x+d) = n_1$ and $n_2(x+d) = n_2$. Here, $d = a+b$ is the period of the lattice, where a and b are the widths of the two regions having refractive indices n_1 and n_2, respectively.

The one-dimensional wave equation for the spatial part of the

electromagnetic eigen mode can be written as

$$\frac{d^2E(x)}{dx^2} + \left[\left(\frac{\omega}{c}n\right)^2 - \beta^2\right] E(x) = 0, \tag{2}$$

where $n(x)$ is given by Eq. (1), and it is assumed to be constant in each region. In this equation, β, ω, c are the propagation constant, frequency, and velocity of light, respectively. Also, $\omega = \frac{2\pi c}{\lambda}$, where λ is the wavelength of light waves. Using Eq. (1), the wave equation can be written separately for the two regions.

In this case, the electric field distribution $E(x)$ within each homogeneous layer can be expressed as the sum of an incident and reflected plane waves. Thus, the electric field in the mth unit cell is given by

$$E(x) = \begin{cases} a_m e^{-ik_1(x-md)} + b_m e^{ik_1(x-md)}; & (md-a) < x < md \\ c_m e^{-ik_2(x-md+a)} + d_m e^{ik_2(x-md+a)}; & (m-1)d < x < (md-a) \end{cases}, \tag{3}$$

where a_m, b_m, c_m, and d_m are constants.

Here, $k_1 = \left[\left(\frac{\omega}{c}n_1\right)^2 - \beta^2\right]^{1/2} = \frac{n_1\omega}{c}\cos\theta_1$, and $k_2 = \left[\left(\frac{\omega}{c}n_2\right)^2 - \beta^2\right]^{1/2} = \frac{n_2\omega}{c}\cos\theta_2$, with θ_1 and θ_2 being the ray angles in the successive layers. If θ is the angle of incidence, then according to the Snell's law, $\cos\theta_1 = \sqrt{1 - \left(\frac{1}{n_1}\right)^2 \sin^2\theta}$ and $\cos\theta_2 = \sqrt{1 - \left(\frac{n_1}{n_2}\right)^2 \sin^2\theta_1}$. By using the matrix multiplication method for TE wave and after simplification, we get the following unit cell translation matrix equation:

$$\begin{pmatrix} a_{m-1} \\ b_{m-1} \end{pmatrix} = \frac{1}{2}\begin{pmatrix} A & B \\ C & D \end{pmatrix}\begin{pmatrix} a_m \\ b_m \end{pmatrix}, \tag{4}$$

where the matrix elements are expressed as

$$\begin{aligned} A &= e^{ik_1a}\left[\cos k_2b + \frac{1}{2}i\left(\frac{k_2}{k_1} + \frac{k_1}{k_2}\right)\sin k_2b\right], \\ B &= e^{-ik_1a}\left[\frac{1}{2}i\left(\frac{k_2}{k_1} - \frac{k_1}{k_2}\right)\sin k_2b\right], \\ C &= e^{ik_1a}\left[-\frac{1}{2}i\left(\frac{k_2}{k_1} - \frac{k_1}{k_2}\right)\sin k_2b\right], \\ D &= e^{-ik_1a}\left[\cos k_2b - \frac{1}{2}i\left(\frac{k_2}{k_1} + \frac{k_1}{k_2}\right)\sin k_2b\right]. \end{aligned}$$

The matrix Eq. (4) will be unimodular since it relates incident and reflected amplitudes of two equivalent layers and hence, $AD-BC=1$. From Floquet theorem, we have $E_K(x,z) = E_K(x)e^{-i\beta z}e^{-iKx}$, where $E_K(x+d) = E_K(x)$. Then, we get $\begin{pmatrix} a_m \\ b_m \end{pmatrix} = e^{-iKd}\begin{pmatrix} a_{m-1} \\ b_{m-1} \end{pmatrix}$, where K is the Bloch wave number. Making use of this relation in Eq. (4), K is obtained from the eigen value of the translation matrix $\begin{pmatrix} A & B \\ C & D \end{pmatrix}$, and can be written as

$$K(\beta,\omega) = \frac{1}{d}\cos^{-1}\left[\frac{1}{2}(A+D)\right] \tag{5}$$

Solving Eq. (5), the dispersion relation between ω and K can be expressed as

$$\cos(Kd) = \cos(k_1a)\cos(k_2b) - \frac{1}{2}\left[\frac{k_2}{k_1}+\frac{k_1}{k_2}\right]\sin(k_1a)\sin(k_2b). \tag{6}$$

Now, the coefficient of reflection of the structure can be derived by using the relation

$$r_{_N} = \begin{pmatrix} b_0 \\ a_0 \end{pmatrix}_{b_{_N}=0} \tag{7}$$

By solving this equation, the coefficient of reflection is given by

$$r_{_N} = \frac{CU_{N-1}}{AU_{N-1}-U_{N-2}},$$

where $U_N = \frac{\sin(N+1)Kd}{\sin(Kd)}$, and N is total number of unit cells. Finally, reflectance (R_N) of the structure is determined by the expression

$$R_{N=}|r_N|^2 = \frac{|C|^2}{|C|^2 + \left(\dfrac{\sin Kd}{\sin NKd}\right)^2}, \tag{8}$$

where C is matrix element.

By using Eq. (8), the reflectance versus wavelength (λ) spectra are plotted for different incident angles with different number of unit cells, and thus reflection spectra are obtained. Also, transmission spectra can be plotted using the relation $T_N = 1-R_N$, if we assume that there

is no absorption of the electromagnetic radiation by the considered crystal.

Further, we employ the analogy of Kronig-Penney model in the band theory of solids with the help of Bloch theorem under the appropriate boundary conditions, we get four differential equations with four unknown constants. Hence, we obtain a determinant of their coefficients of the order 4×4. For nontrivial solution to exist the determinant so formed must vanish, and its solution gives

$$\cos(Kd) = \cos(k_1 a)\cos(k_2 b) - \frac{1}{2}\left[\frac{n_2}{n_1} + \frac{n_1}{n_2}\right]\sin(k_1 a)\sin(k_2 b), \quad (9)$$

where $k_1 = \frac{n_1\omega}{c}$ and $k_2 = \frac{n_2\omega}{c}$. Here, we find that, for normal incidence ($\beta = 0$), the dispersion relation (6) derived using the transfer matrix approach reduces to Eq. (9) as determined by the Kronig-Penney model. We rewrite the Eq. (6) as

$$\cos(k_1 a)\cos(k_2 b) - \frac{1}{2}\left[\frac{k_2}{k_1} + \frac{k_1}{k_2}\right]\sin(k_1 a)\sin(k_2 b) = \cos(Kd) \quad (10)$$

If we abbreviate the left-hand side (LHS) of Eq. (10) as L, then

$$L = \cos(Kd), \quad (11)$$

and

$$L = \cos(k_1 a)\cos(k_2 b) - \frac{1}{2}\left[\frac{k_2}{k_1} + \frac{k_1}{k_2}\right]\sin(k_1 a)\sin(k_2 b). \quad (12)$$

Thus, with the help of Eq. (12), we can draw L versus λ curves at different incident angles, and forbidden bands are obtained with the analogy of Kronig-Penney model. These curves are compared with those reflection spectra obtained using the matrix formulation approach (8) at different incident angles, and some conclusions are drawn.

3. RESULTS AND DISCUSSION

In this section, we analyze the effect of variation of incident angle on the reflectivity of a nanolayered structure with different number of unit cells. We obtain the reflection spectra for different cases with the help of Eq. (8). For the proposed photonic crystal, we have chosen $n_1 = 1$ (air), $n_2 = 3.6$ (GaAs); $a = 250\,\text{nm}$, and $b = 160\,\text{nm}$. To study the reflection properties of the photonic crystal, we have considered different number of unit cells: $N = 5$, 10, 17, and angle of incidence

is varied as: $\theta = 0°$, $30°$, $45°$ and $60°$. We plot the reflectance versus wavelength spectra for these unit cells at four different incident angles. Further, by using Eq. (12), L versus λ curves are drawn at these four incident angles.

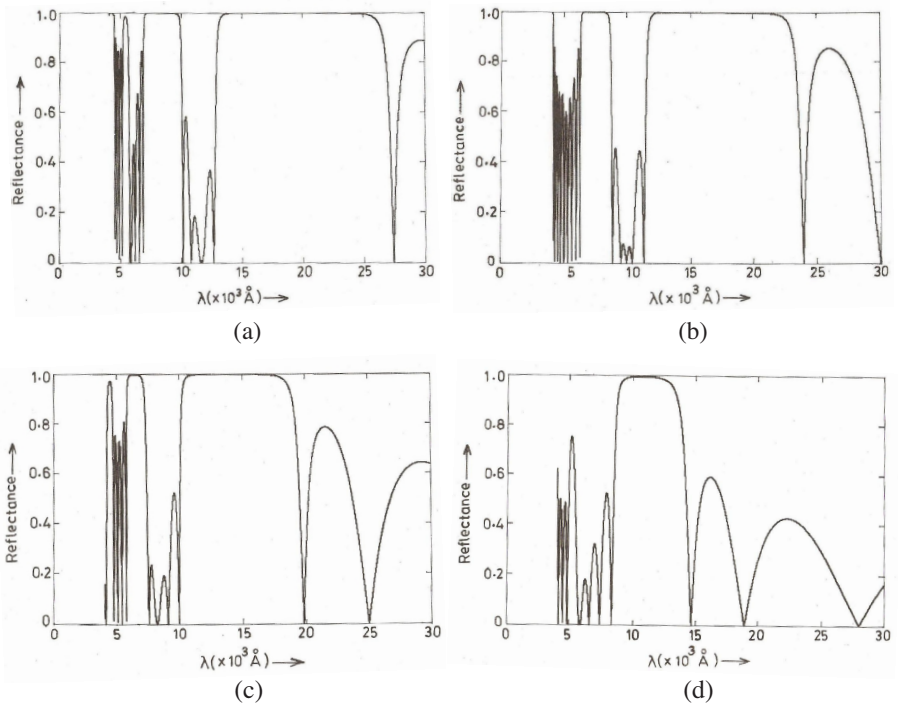

Figure 2. (a) Reflectivity spectrum for $N = 5$ at normal incidence ($\theta = 0°$), (b) reflectivity spectrum for $N = 5$ and $\theta = 30°$, (c) reflectivity spectrum for $N = 5$ and $\theta = 45°$, (d) reflectivity spectrum for $N = 5$ and $\theta = 60°$.

Figures 2(a)–(d), 3(a)–(d), and 4(a)–(d) represent the reflection spectra of the photonic crystal for$N = 5$, 10 and 17, respectively. Figures 4(e)–(h) show the transmission spectra for $N = 17$ assuming the media as absorption less. In this study, we have focussed our attention to the completely reflected ($\approx 100\%$) bands of the reflection spectra in visible and infrared regions. It is observed from these reflection spectra in different cases that the first broadband of completely reflected range of wavelength exists in a small portion of the visible region, whereas the second broadband lies in a larger width of the infrared (IR) regime. Thus, we find that, wide ranges of infrared and shorter width of visible regions are completely reflected.

The obtained results are listed in Tables 1–3. It reveals that the proposed photonic crystals with different unit cells are perfect infrared broadband reflectors.

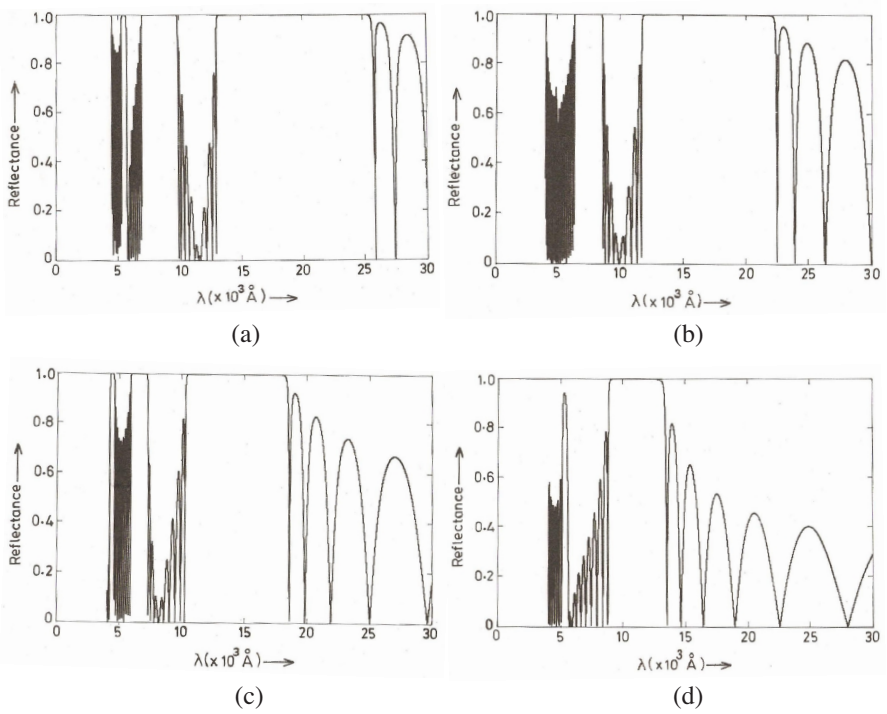

Figure 3. (a) Reflectivity spectrum for $N = 10$ at normal incidence ($\theta = 0°$), (b) reflectivity spectrum for $N = 10$ and $\theta = 30°$, (c) reflectivity spectrum for $N = 10$ and $\theta = 45°$, (d) reflectivity spectrum for $N = 10$ and $\theta = 60°$.

Table 1. Reflection range for $N = 5$ at different incident angles.

Angle of Incidence (θ) (degree)	Complete Reflection (≈100%) Range ($A°$)	
	First Broadband	Second Broadband
0	7124–9411	14287–23015
30	6670–8071	13048–19550
45	6151–6637 (≈ 99.8%)	12013–15152
60	< 80%	10024–13398 (≈ 99.6%)

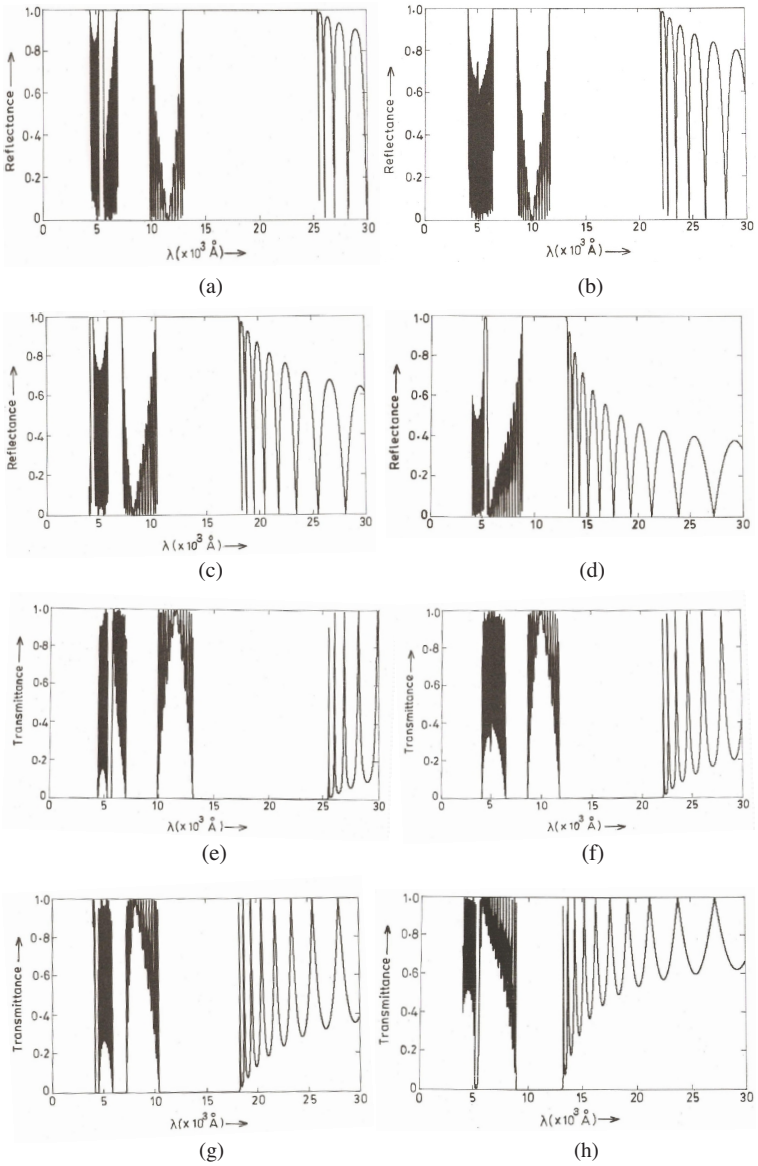

Figure 4. (a) Reflectivity spectrum for $N = 17$ at normal incidence ($\theta = 0°$), (b) reflectivity spectrum for $N = 17$ and $\theta = 30°$, (c) reflectivity spectrum for $N = 17$ and $\theta = 45°$, (d) reflectivity spectrum for $N = 17$ and $\theta = 60°$, (e) transmitivity spectrum for $N = 17$ at normal incidence ($\theta = 0°$), (f) transmitivity spectrum for $N = 17$ and $\theta = 30°$, (g) transmitivity spectrum for $N = 17$ and $\theta = 45°$, (h) transmitivity spectrum for $N = 17$ and $\theta = 60°$.

Table 2. Reflection range for $N = 10$ at different incident angles.

Angle of Incidence (θ) (degree)	Complete Reflection ($\approx 100\%$) Range (A°)	
	First Broadband	Second Broadband
0	6962–9794	13262–25105
30	6464–8544	11959–21761
45	5933–7059	10564–17801
60	5226–5292 ($< 99.5\%$)	09210–12587

Table 3. Reflection range for $N = 17$ at different incident angles.

Angle of Incidence (θ) (degree)	Complete Reflection ($\approx 100\%$) Range (A°)	
	First Broadband	Second Broadband
0	6945–9847	13128–25328
30	6428–8611	11829–22007
45	5889–7165	10427–18088
60	5228–5310 ($\approx 99.4\%$)	08973–13033

Figures 5(a)–(d) illustrate the variation of the LHS of Eq. (12) as a function of wavelength (λ) for different incident angles. With the analogy of Kronig-Penney model, since the right-hand side (RHS) of Eq. (11) is a cosine function, the allowed values in L versus λ plots will lie between the range -1 to $+1$. However, the portions of the curve lying beyond these limiting values are forbidden ranges of λ. The forbidden bands are mentioned in Table 4.

The above results so obtained are compared and some insights are drawn. The comparison between the reflection spectra in different cases shows that, as the number of layers is increased, the reflectivity of the photonic crystal increases. We get the maximum reflectance for $N = 17$ and further by increasing the number of layers, it can be shown that the reflectivity of the structure will be almost saturated [15, 18]. However, the completely reflected bandwidth (A°) in all cases of unit cell decreases with increase in the angle of incidence. The suggested infrared broadband reflectors provide complete reflectance for a limited set of incident angles 0° to 45°, and if we further increase the angle, reflectivity decreases significantly. Here, the largest reflected

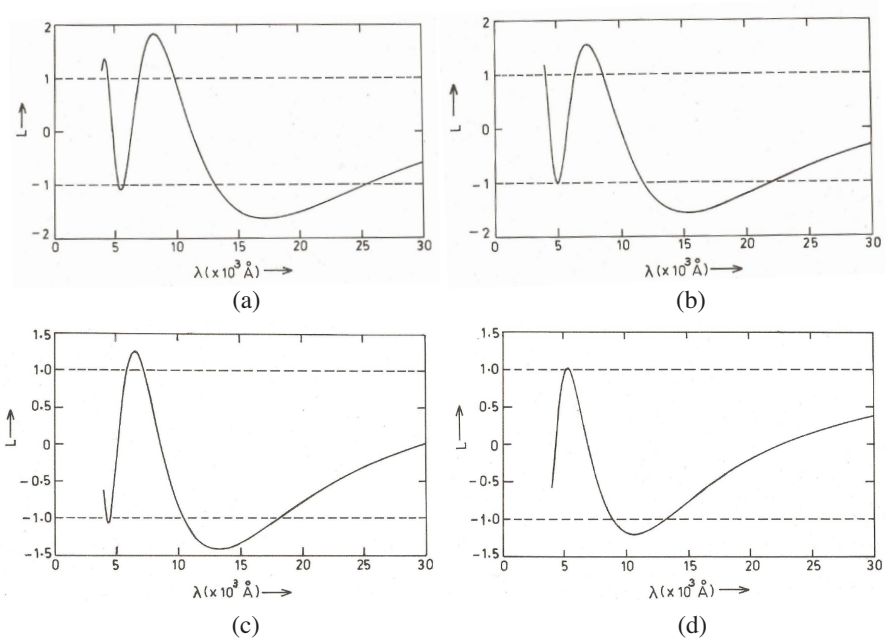

Figure 5. (a) Variation of L with wavelength (λ) at normal incidence ($\theta = 0°$), (b) variation of L with wavelength (λ) at $\theta = 30°$, (c) variation of L with wavelength (λ) at $\theta = 45°$, (d) variation of L with wavelength (λ) at $\theta = 60°$.

bandwidth is obtained for the normal incidence ($\theta = 0°$). In addition, the completely reflected bands are shifted towards lower wavelength side with increase in the incident angle. Thus, angle of incidence can be considered as a controlling factor for the reflection properties of the photonic crystals.

Table 4. Forbidden broadbands at different incident angles.

Angle of Incidence (θ) (degree)	Forbidden Broadband ($A°$)	
	First Broadband	Second Broadband
0	6944–9859	13092–25337
30	6426–8628	11796–22033
45	5882–7196	10394–18137
60	5177–5440	08917–13142

Furthermore, we compare the completely reflected broadbands shown in Figures 2–4 for different incident angles with the forbidden bands those obtained by using the analogy of Kronig-Penney model as depicted in Figures 5(a)–(d). We observe that the completely reflected ranges of wavelength for different incident angles mentioned in Tables 1–3 correspond to the forbidden ranges shown in Table 4, which shows that these ranges are in good agreement. It indicates that the completely reflected ranges are forbidden bandgap, i.e., stop bands, where no propagation takes place. This is shown as an important feature of the proposed photonic crystals.

In conclusion, the proposed photonic crystals with specified values of the lattice parameters and different unit cells are broadband reflectors within the infrared region of electromagnetic radiation, and angle of incidence acts as a controlling factor for their reflection properties. Also, the completely reflected bands lie in the visible region. Hence, these photonic crystals can be used as wavelength selective mirrors. Moreover, it can also be made possible to obtain a larger bandwidth of the visible spectrum completely reflected from the structure by tuning the values of lattice parameters. Such suggested mirrors offer much low loss as compared to the case of reflectors using metallic counterparts. This theoretical analysis may have some technological applications in integrated optics, and fabrication of photonic devices such as optical filters.

ACKNOWLEDGMENT

One of the authors (N. Kumar) is thankful to Department of Applied Physics, Institute of Technology, Banaras Hindu University, India. Thanks are also due to Dr. Shakti Baijal, MITS, Lakshmangarh, for her support.

REFERENCES

1. Joannopoulos, J. D., R. D. Meade, and J. N. Winn, *Photonic Crystals: Modeling the Flow of Light*, Princeton University Press, NJ, 1995.
2. Dowling, J. P. and C. M. Bowden, "Anomalous index of refraction in photonic band gap materials," *J. Mod. Optics*, Vol. 41, 345–351, 1994.
3. Kosaka, H., T. Kawashima, A. Tomita, T. Sato, and S. Kawakami, "Photonic crystal spot-size convertor," *Appl. Phys. Lett.*, Vol. 76, 268–270, 2000.

4. Joannopoulus, J. D. and E. F. Schubert, "High extraction efficiency of spontaneous emission from slabs of photonic crystals," *Phy. Rev. Lett.*, Vol. 78, 3294, 1997.
5. Meade, R. D., K. D. Bromer, J. D. Joannopoulos, and O. L. Alerhand, "Accurate theoretical application of photonic band gap materials: Low loss bends and high Q cavities," *J. Appl. Phys.*, Vol. 75, 4753–4755, 1994.
6. Papalakis, E., N. J. Kylstra, and P. L. Knight, "Transparency near a photonic band edge," *Am. Phys. Soc.*, 34–36, 1999.
7. Pendry, J., "New electromagnetic materials emphases the negative," *Physics World*, 1–5, 2001.
8. Yablonovitch, E., "Inhibited spontaneous emission in solid-state physics and electronics," *Phys. Rev. Lett.*, Vol. 58, 2059–2062, 1987.
9. Knight, J. C., J. Arriage, T. A. Birks, A. O. Blanch, W. J. Wadsworth, and P. S. J. Ruseel, "Anomalous dispersion in photonic crystal fiber," *IEEE, Photon. Tech. Lett.*, Vol. 12, 807–809, 2000.
10. Jia, V. and K. Yasumoto, "Modal analysis of two dimensional photonic crystal waveguide formed by rectangular cylinders using an improved Fourier series method," *IEEE, Trans. Microwave Theory and Techniques*, Vol. 54, 564–567, 2006.
11. Srivastava, S. K., S. P. Ojha, and K. S. Ramesh, "Design of an ultraviolet filter based on photonic bandgap materials," *Microwave Opt. Technol. Lett.*, Vol. 33, 308–314, 2002.
12. Ojha, S. P., S. K. Srivastava, N. Kumar, and S. K. Srivastava, "Design of an optical filter using photonic band gap material," *Optik*, Vol. 114, 101–105, 2003.
13. Fink, Y., J. N. Winn, S. Fan, C. Chen, J. Michel, J. D. Joannopoulos, and E. Thomas, "A dielectric omnidirectional reflector," *Science*, Vol. 282, 1679–1682, 1998.
14. Fan, S., P. R. Villeneuve, and J. D. Joannopoulos, "Large omnidirectional bandgaps in metallo dielectric photonic crystals," *Phy. Rev. B*, Vol. 54, 11245, 1996.
15. Yeh, P., *Optical Waves in Layered Media*, John Wiley and Sons, New York, 1988.
16. Yeh, P., A. Yariv, and C.-S. Hong, "Electromagnetic wave propagation in periodic stratified media, I. General theory," *Opt. Soc. Am.*, Vol. 67, 423–437, 1977.
17. Lidoriks, E. and C. M. Soukoulis, "Pulse-driven switching in one-dimensional nonlinear photonic bandgap materials: A numerical

study," *Phys. Rev. E*, 5825–5829, 2000.

18. Kumar, N., "Novel aspects of modal propagation characteristics of some optical waveguides with new geometrical structures and refractive index profiles," Ph.D. Thesis, Appl. Phys., IT, BHU, India, 2002.
19. Kumar, N., S. K. Srivastava, and S. P. Ojha, "A theoretical analysis of the propagation characteristics of an annular circular waveguide with helical winding as the inner cladding," *Microwave and Opt. Technol. Lett.*, Vol. 69, 69–74, 2003.
20. Birks, T., T. Knight, and J. Russel, "Endlessly single mode photonic crystal fiber," *Opt. Lett.*, Vol. 22, 961–963, 1997.
21. Noda, S., "Teaching light new tricks," *Spie OE Magazine*, 28–31, 2001.
22. Ren, H., C. Jiang, W. Hu, M. Gao, and J. Wang, "Photonic crystal channel drop filter with a wavelength selective microcavity," *Optics Express*, Vol. 14, 2446–2458, 2006.
23. Satao, S.-L., J. Wu, and Y.-L. Her, "Triangular finite element analysis of a trapezoid polymer optical waveguide," *Microwave and Optical Technol. Lett.*, Vol. 15, 87–89, 1997.
24. Temelkuran, B., B. Mehmet, E. Ozbay, J. P. Kavanaugh, M. M. Sigalas, and G. Tuttle, "Quasi metallic silicon micromachined photonic crystals," *Appl. Phys. Lett.*, Vol. 78, 264–266, 2001.
25. Shawn, L. Y., J. G. Flemming, R. Robin, M. M. Sigalas, R. Biswas, and K. M. Ho, "Complete three-dimensional photonic bandgap in single cubic structure," *J. Opt. Soc. Am. B*, Vol. 18, 32–35, 2001.
26. Massaoudi, S., A. De lustrac, and I. Huynen, "Properties of metallic photonic bandgap material with defect at microwave frequencies: Calculation and experimental verification," *J. Electromagnetic Waves and Applications*, Vol. 20, 1967–1980, 2006.
27. Villa-Villa, F., J. Gaspar-Armenta, and A. Mendoza-Suár, "Surface modes in one dimensional photonic crystals that include left handed materials," *J Electromagnetic Waves and Applications*, Vol. 21, 485–499, 2007.
28. Singh, S. K., J. P. Pandey, K. B. Thapa, and S. P. Ojha, "Structural parameters in the formation of omnidirectional high reflectors," *Progress In Electromagnetics Research*, PIER 70, 53–78, 2007.

29. Pandey, P. C., A. Mishra, and S. P. Ojha, "Modal dispersion characteristics of a single mode dielectric optical waveguide with a guiding region cross-section bounded by two involuted spirals," *Progress In Electromagnetics Research*, PIER 73, 1–13, 2007.
30. Osipov, A. V., I. T. Iakubov, A. N. Lagarkov, S. A. Maklakov, D. A. Petrov, K. N. Rozanov, and I. A. Ryzhikov, "Multi-layered Fe films for microwave applications," *PIER Online*, Vol. 3, 1303–1306, 2007.
31. Shi, S. and D. W. Prather, "Lasing dynamics of a novel silicon photonic crystal cavity," *PIER Online*, Vol. 3, 746–750, 2007.
32. Yatsyk, V., "Effects of the resonant scattering of Intensive fields by weakly nonlinear dielectric layer," *PIER Online*, Vol. 3, 524–527, 2006.
33. Brongersma, M. L., R. Zia, and J. Schuler, "Plasmonics — The missing link between nanoelectronics and microphotonics," *PIER Online*, Vol. 3, 360–362, 2007.
34. Huang, T.-Y., Y.-C. Yu, and R.-B. Wu, "Dual-band/broadband circular polarizers designed with cascaded dielectric spectrum loading," *PIER Online*, Vol. 2, 475–477, 2007.
35. Lin, M.-C. and R.-F. Jao, "Fnite element analysis of photon densiy states for two-dimensional photonic crystals in plane light propagation," *PIER Online*, Vol. 3, 315–319, 2007.
36. Hou, S. and C. Hu, "Influence ofelectro-optic effecton waveguide efficiency of optical fiber with cladding made of uniaxial crystal materials," *PIER Online*, Vol. 2, 614–618, 2006.
37. Li, L., C.-H. Liang, and C. H. Chan, "Waveguide end slot phased array antenna integrated with electromagnetic bandgap structures," *J. Electromagnetic Waves and Applications*, Vol. 21, 161–174, 2007.
38. Kokkorakis, G. C., "Calculating the electric field in nanostructures," *J Electromagnetic Waves and Applications*, Vol. 21, 1433–144, 2007.